Supplementary Information

Enhancing iodine capture through a zirconium-based metal-organic cage featuring functionalized indole units

Shungang Yang, Zhengyang Wu, Kang Wang, Nan Wei, Yanyan Feng, Peng Cui, Yao Jiang*

School of Chemistry and Chemical Engineering, Hefei University of Technology, Hefei 230009, China

Email: yjiang@hfut.edu.cn

Materials

1H-Indole-2,5-dicarboxylic Acid， Iodine (I_2) and Cp_2ZrCl_2 were purchased from Shanghai Titan Technology Co., LTD. 1,4-Dioxane, acetonitrile, acetone, and cyclohexane were purchased from Shanghai Aladdin Biochemical Technology Co., LTD. All reagents were commercially available products and used without further purification.

Characterization

High-resolution electrospray ionization time-of-flight mass spectrometry (ESI-TOF-MS) was performed on a Vanquish Q Exactive Plus instrument from Thermo Fisher. Scanning electron microscopy (SEM), corresponding elemental mapping analysis, and energy-dispersive X-ray spectroscopy (EDS) analysis were conducted using a Regulus 8230 electron microscope operated at 2 kV. ^{1}H nuclear magnetic resonance (NMR) spectra were recorded on a Bruker AVANCE NEO-600 MHz instrument. Fourier transform infrared (FTIR) spectroscopy was performed on a ThermoFisher Nicolet iS10 spectrometer with samples diluted in KBr pellets. X-ray photoelectron spectroscopy (XPS) analysis was carried out on a Thermo Scientific ESCALAB 250Xi instrument. Raman spectra were recorded on a LabRAM HR Evolution instrument with 532 nm excitation wavelength. Thermogravimetric analysis (TGA) was conducted on a TG209F1 instrument, where samples were heated from room temperature to 1000 °C at 10 °C·min^{-1} under N_2 atmosphere. UV-vis spectra were recorded on a Shimadzu UV2550 spectrophotometer using quartz cells (10 mm optical path length). Single crystal diffraction data was collected on a ROD, synergy custom DW system equipped with a HyPix-Arc 150 diffractometer. The crystal was maintained at 100.00(10) K during data collection. Using Olex2,[1] the structure was solved with the SHELXT program through intrinsic phasing and refined with the SHELXL package using least-squares minimization.[2,3]

Synthesis of Zr-MOC-Indole

For the synthesis of Zr-MOC-Indole, 1H-Indole-2,5-dicarboxylic Acid (6.0 mg, 0.029

mmol), Cp_2ZrCl_2 (17.5 mg, 0.059 mmol), 1 mL of 1,4-dioxane, and 0.5 mL of acetonitrile were combined in a 3 mL glass vial. The mixture was sonicated until all solids were dissolved, and then 5 drops of H_2O were added. The resulting solution was incubated at 60 °C for 10 hours. Rod-shaped crystals of Zr-MOC-Indole formed and were subsequently washed with 1,4-dioxane and acetone. The crystals were then vacuum-dried at 50 °C for 12 h, yielding a white powder. The overall yield of the synthesis was approximately 87%.

Iodine adsorption experiment

In the iodine adsorption experiments, 30 mg of Zr-MOC-Indole was accurately weighed and placed in a 5 mL glass vial. This vial was then inserted into a 50 mL glass vial containing iodine granules. The 50 mL vial was sealed and heated to 75 °C under standard pressure. At predetermined time intervals, the 5 mL vial containing the Zr-MOC-Indole sample was removed, allowed to cool, carefully cleaned, and reweighed. The increase in mass was recorded before the vial was returned to the 50 mL vial. The iodine vapor uptake capacity was calculated using the following formula:

$$M_t = \frac{m_t - m_0}{m_0} \tag{1}$$

where M_t represents the iodine uptake per gram of adsorbent at time t (h), while m_0 and m_t denote the mass of Zr-MOC-Indole before and after exposure to iodine vapor, respectively. Additionally, the experiment was conducted three times to ensure consistency.

The pseudo-first-order (2), pseudo-second-order (3) were employed according to the following equations:

$$\log(q_e - q_t) = \log q_e - \frac{k_1}{2.303} t \tag{2}$$

$$\frac{t}{q_t} = \frac{1}{k_2 q_e^2} + \frac{t}{q_e} \tag{3}$$

where q_e ($g \cdot g^{-1}$) and q_t ($g \cdot g^{-1}$) represent the uptake amount at equilibrium stage and time t (h), respectively; k_1 and k_2 denote the pseudo-first-order and pseudo-second-order

kinetic rate constants.

To collect the data of iodine uptake capacity from I_2/cyclohexane solution, an experiment was conducted by taking 30 mg of Zr-MOC-Indole and added to 3 mL of 300 ppm I_2/cyclohexane solution. At different time intervals, the supernatants were taken, and their UV-vis spectra was recorded. The concentration is determined from the UV-Vis spectral standard curve of different concentrations of iodine/cyclohexane solutions. The percentage of iodine captured was determined using the formula:

$$removal = \frac{C_0 - C_t}{C_0} \times 100\% \quad (4)$$

where C_0 and C_t are the initial concentration in I_2/cyclohexane solution at the start of the experiment and at time t, respectively.

Theoretical calculation

This study employed periodic first-principles calculations based on density functional theory (DFT) as implemented in the CP2K software package.[4] All calculations utilized the PBE functional under the generalized gradient approximation (GGA), with Grimme's DFT-D3 method incorporating BJ-damping for dispersion correction.[5] The plane-wave cutoff energy was set to 500 eV, and the k-point grid was configured using the Monkhorst-Pack scheme with dimensions of 2 × 2 × 2. The convergence criteria for geometric optimization were set as follows: forces on atoms less than 0.03 eV/Å and energy changes below 1.0×10^{-5} eV/atom. The TZVP-MOLOPT-GTH basis set was employed for C, H, O, and N atoms. For the Zr atom, the TZVP-MOLOPT-GTH basis set was used, and for the I atom, the DZVP-MOLOPT-GTH basis set was adopted, both with their corresponding GTH pseudopotentials that account for scalar relativistic effects.[6] The electrostatic potential (ESP) distribution was analyzed based on the optimized framework structure, and the charge density difference before and after adsorption was calculated to visually reveal the rearrangement of electron density. The binding energies (ΔE) between Zr-MOC-Indole and iodine species were calculated by $\Delta E = E_{\text{iodine@Zr-MOC-Indole}} - E_{\text{Zr-MOC-Indole}} - E_{\text{iodine}}$.

Crystallographic refinement details for Zr-MOC-Indole

1. Explicitly report the solvent mask result of ~503 electrons per ASU.
2. State that this electron count is consistent with the presence of approximately ten 1,4-dioxane molecules, one acetonitrile, and one water molecule in the crystal voids, alongside the two chloride counterions.
3. Clearly explain that the explicitly modelled solvent molecules represent the major ordered components, while the total electron density includes contributions from additional, highly disordered solvent species that are treated statistically by the mask procedure.

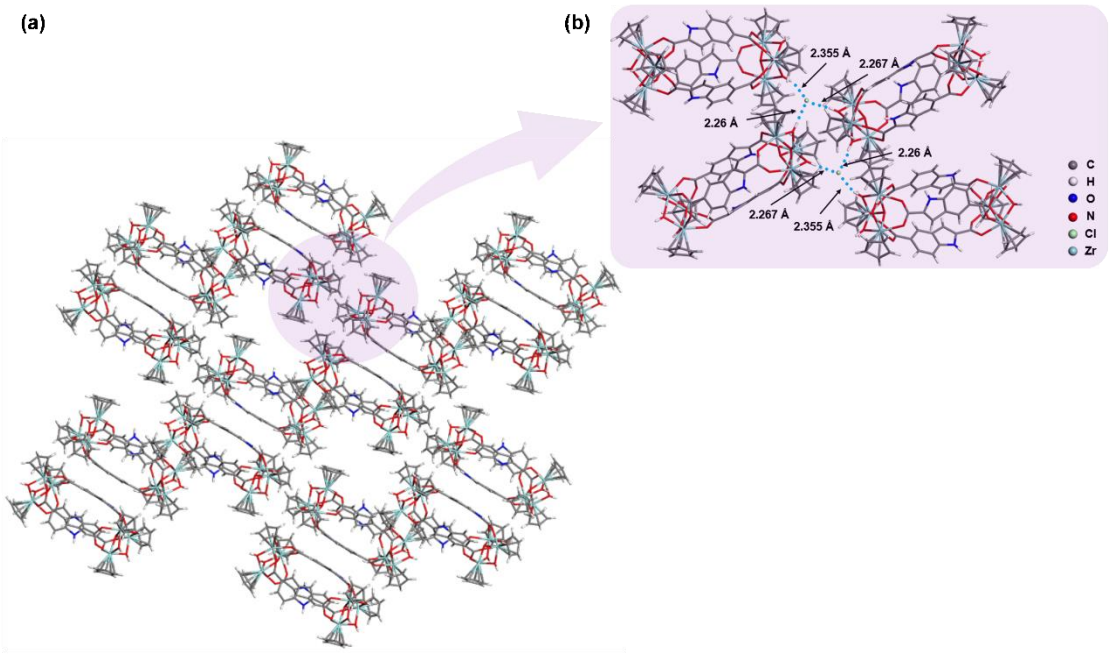

Fig. S1. (a) The packing modes for the crystal of Zr-MOC-Indole. (b) The arrangement of cages with hydrogen bond connections in Zr-MOC-Indole.

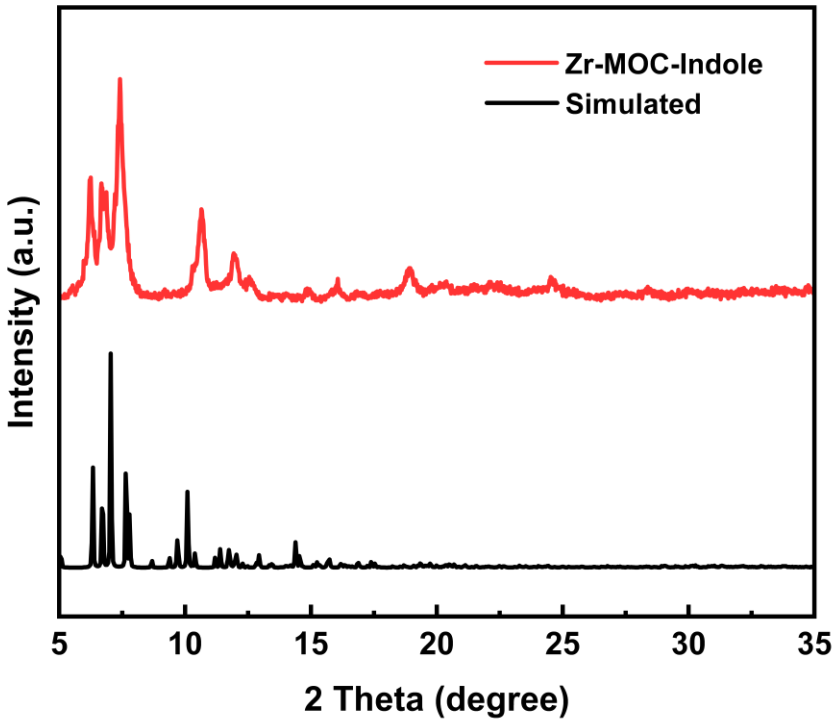

Fig. S2. PXRD patterns of Zr-MOC-Indole.

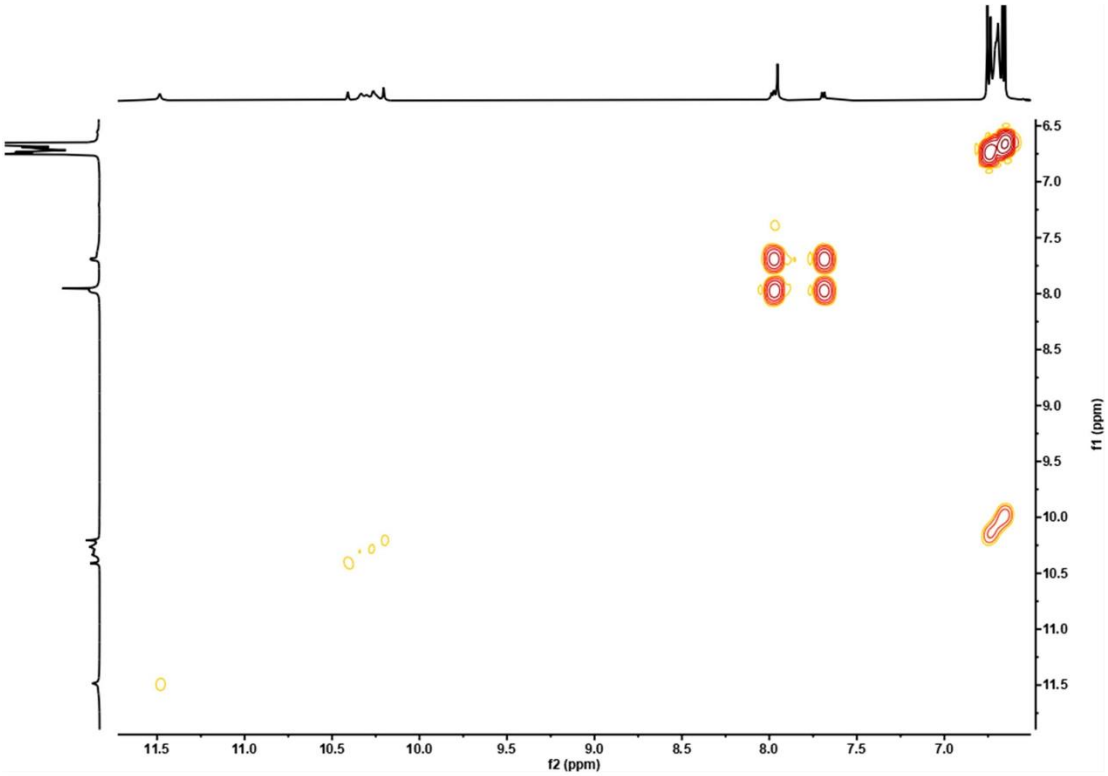

Fig. S3. ^{1}H COSY spectrum of Zr-MOC-Indole.

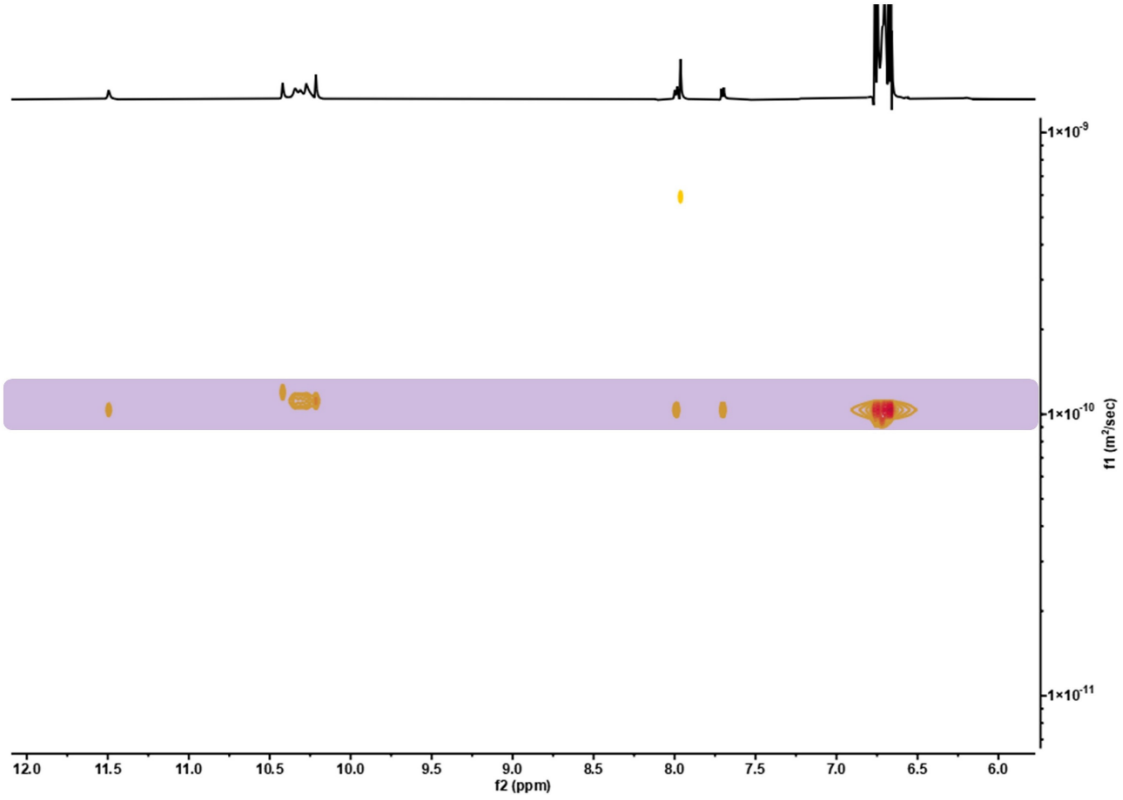

Fig. S4. ^{1}H DOSY spectrum of Zr-MOC-Indole.

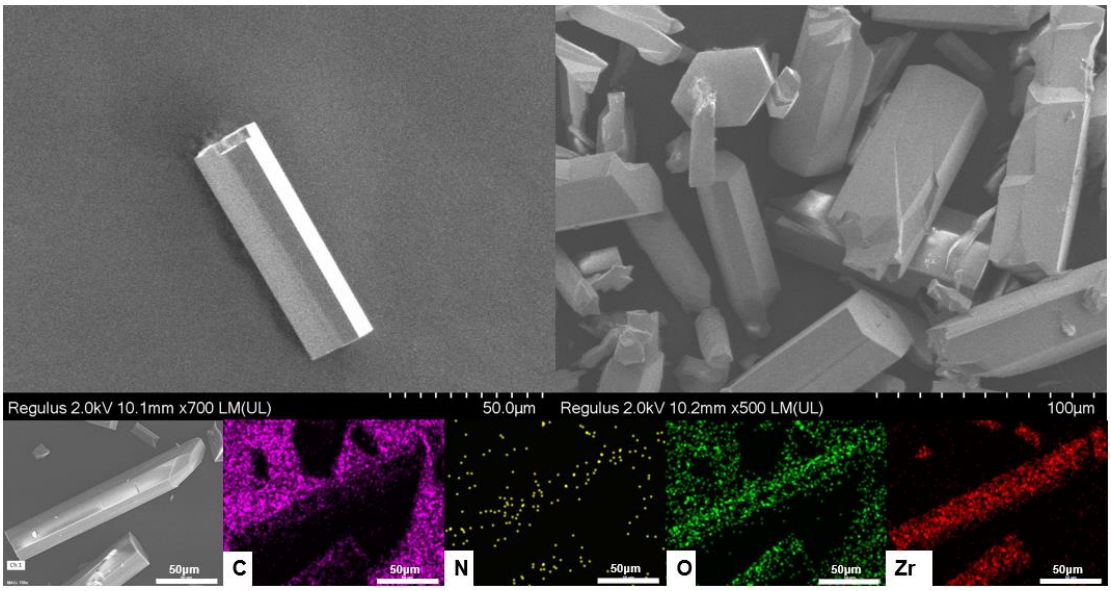

Fig. S5. SEM and elemental-mapping images of Zr-MOC-Indole.

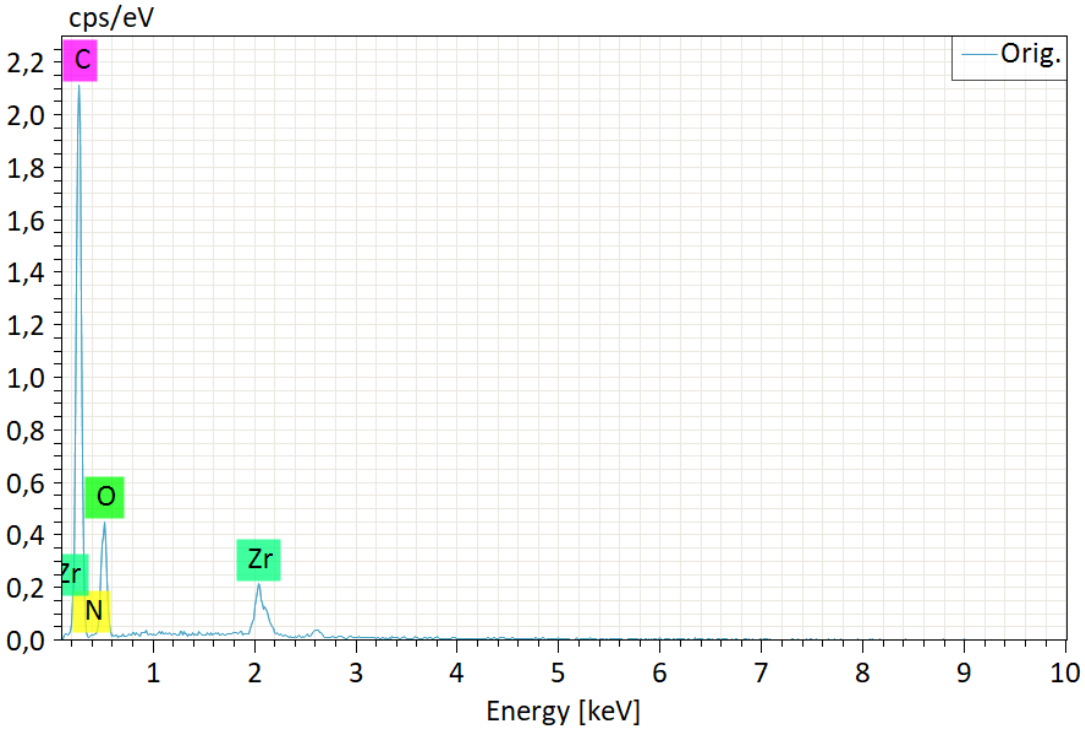

Fig. S6. EDS spectrum of Zr-MOC-Indole.

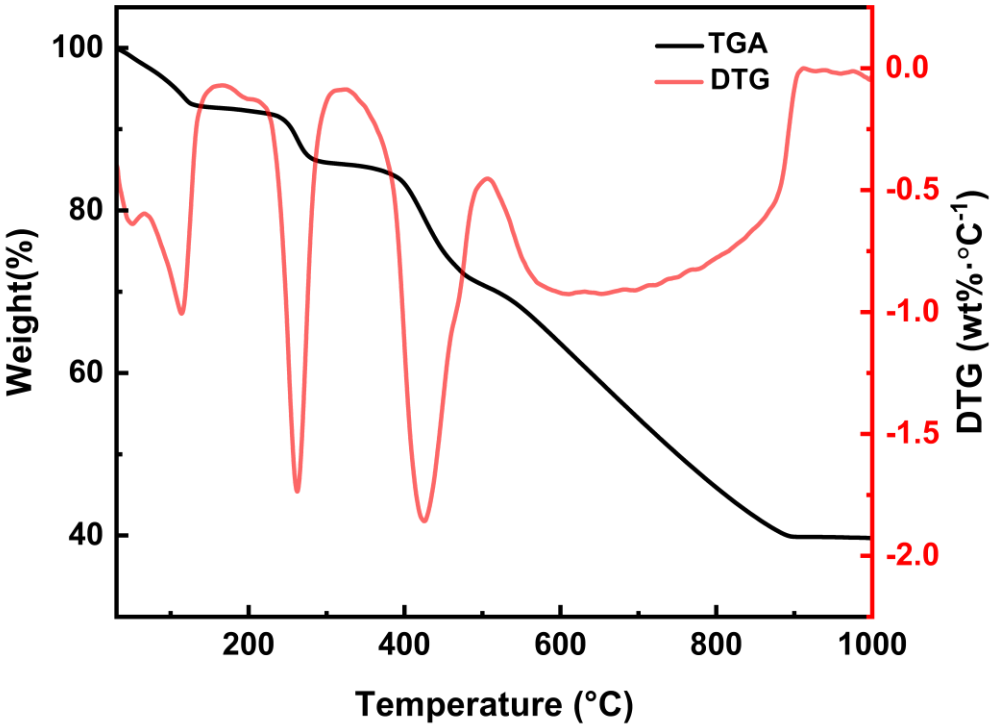

Fig. S7. TGA and DTG curves of Zr-MOC-Indole.

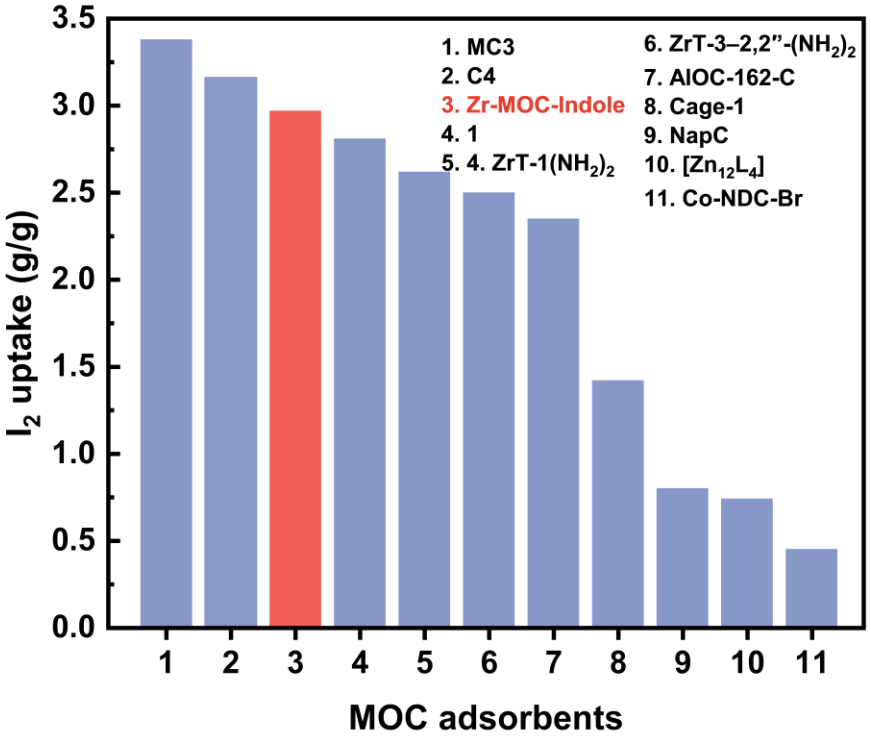

Fig. S8. Iodine vapor adsorption capacities of different MOC-based adsorbents[7-13].

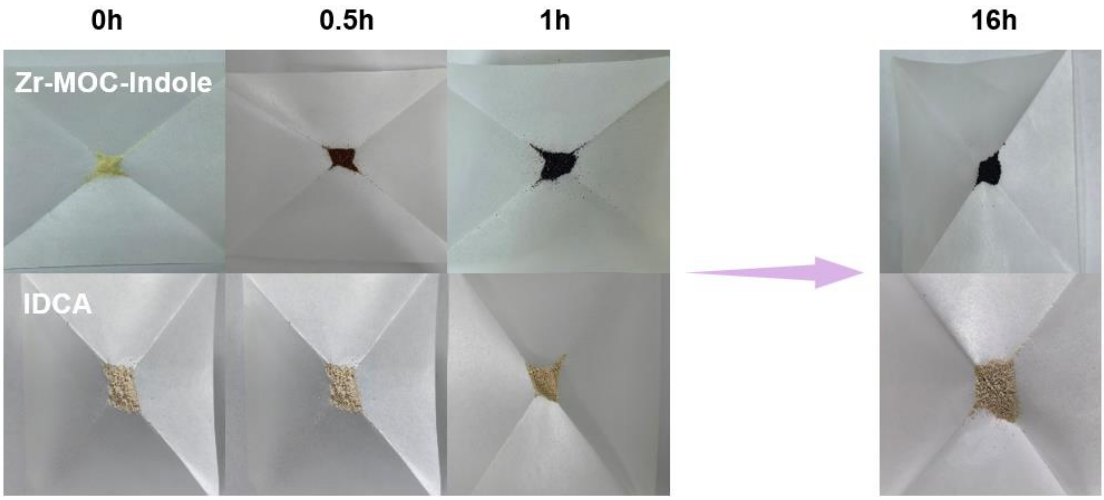

Fig. S9. Color change diagrams of Zr-MOC-Indole and ligand 1H-indole-2,5-dicarboxylic acid (IDCA) during iodine vapor adsorption.

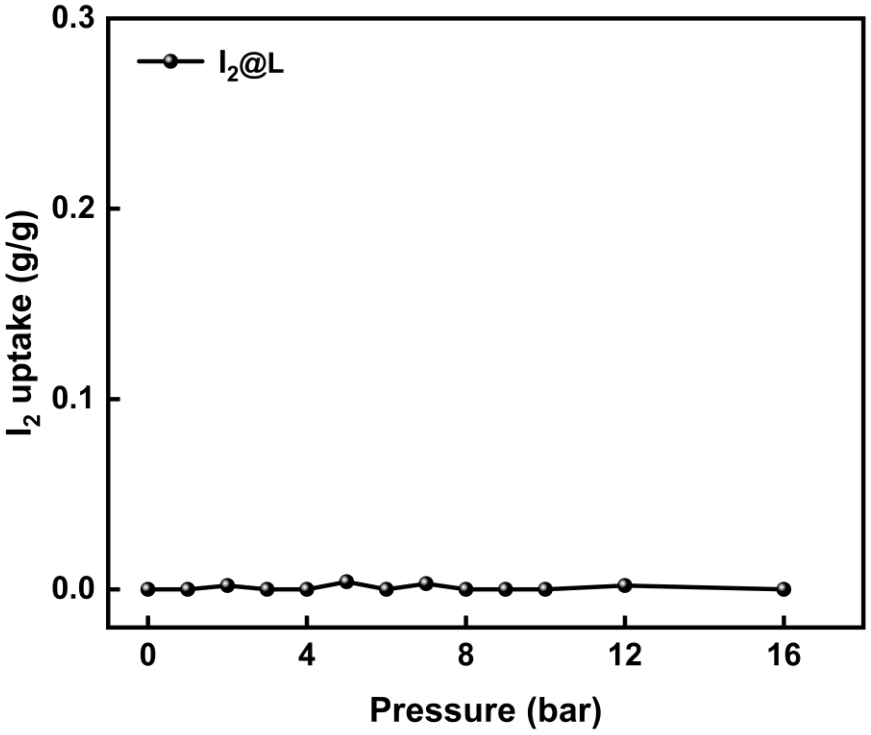

Fig. S10. Time-dependent iodine uptake plots for 1H-indole-2,5-dicarboxylate at 75 °C.

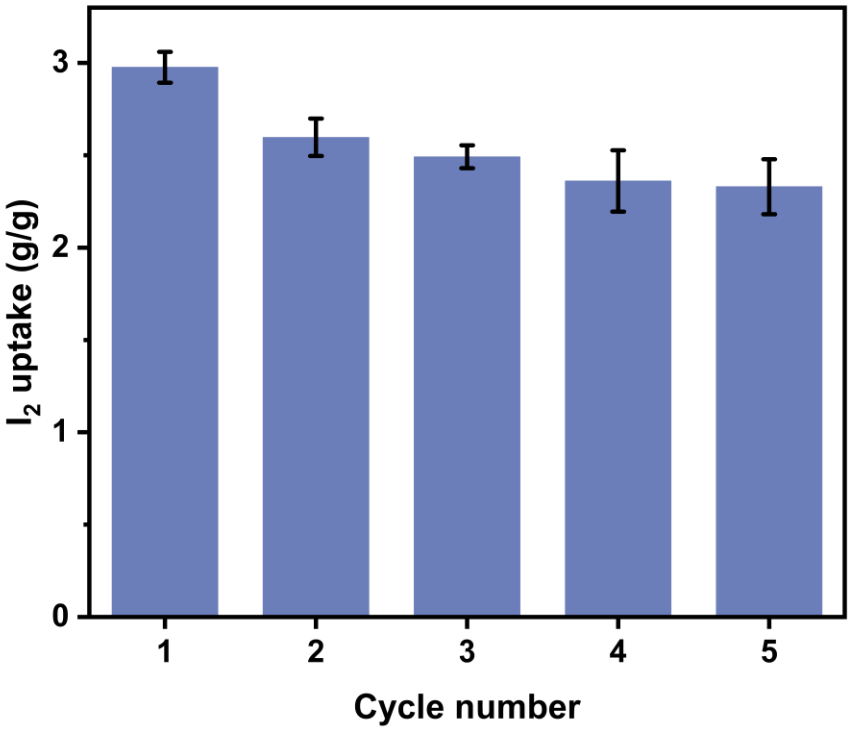

Fig. S11. Iodine vapor adsorption capacities on Zr-MOC-Indole in five cycles.

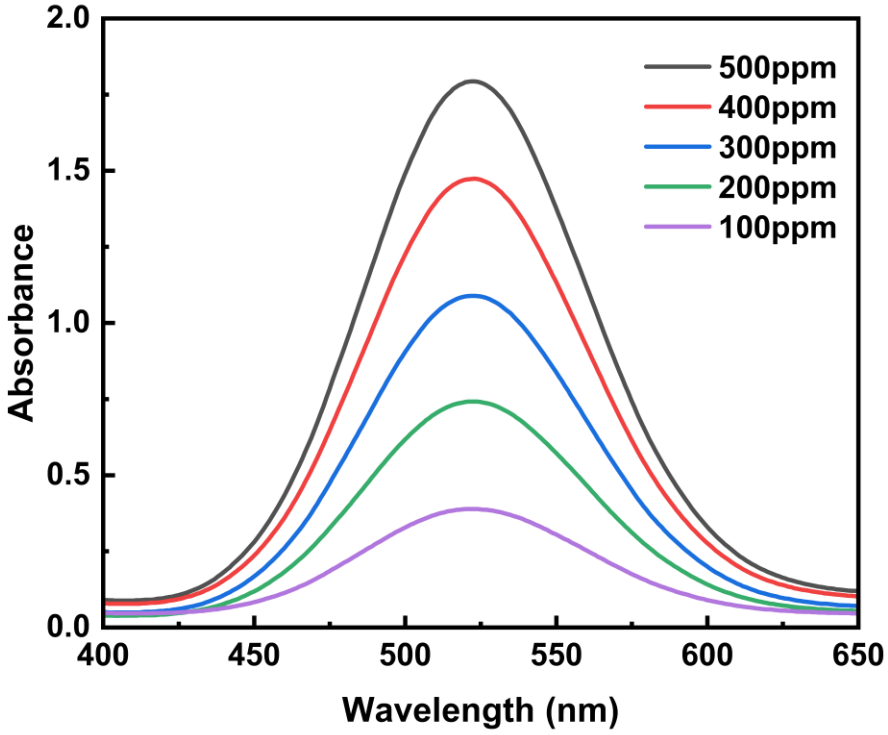

Fig. S12. UV-vis spectra of different concentrations of iodine/cyclohexane solutions.

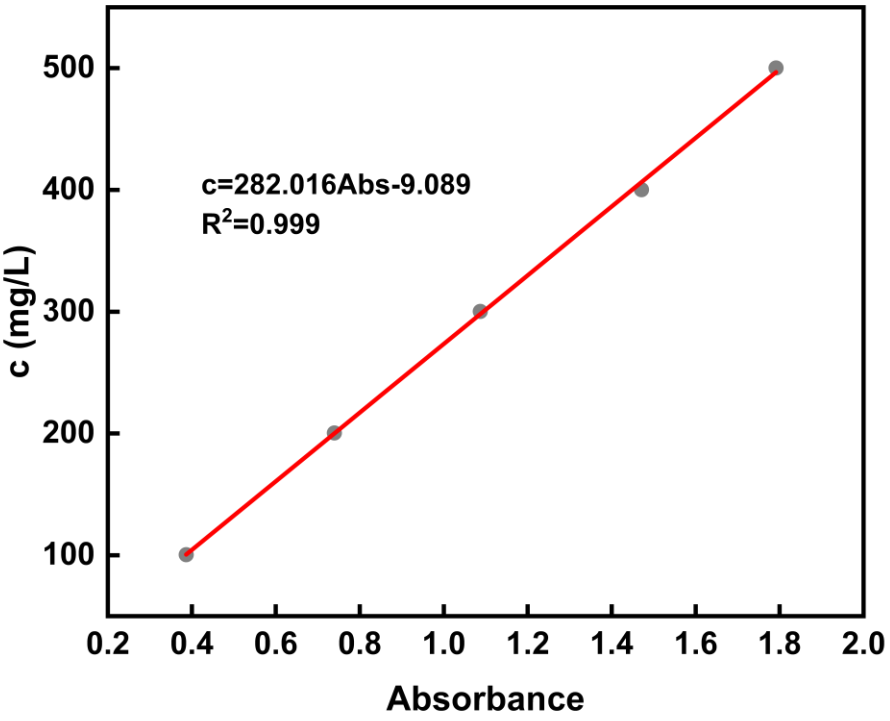

Fig. S13. UV-vis spectral standard curve of iodine in cyclohexane.

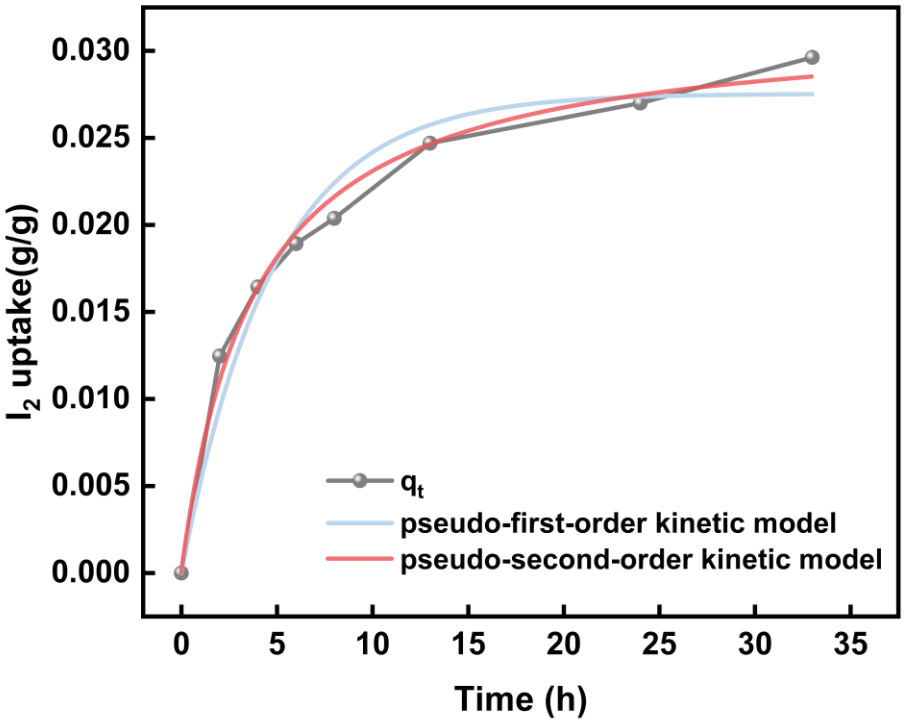

Fig. S14. The pseudo-first-order and pseudo-second-order kinetic data of the iodine adsorption in iodine/cyclohexane solutions (300 ppm) by Zr-MOC-Indole.

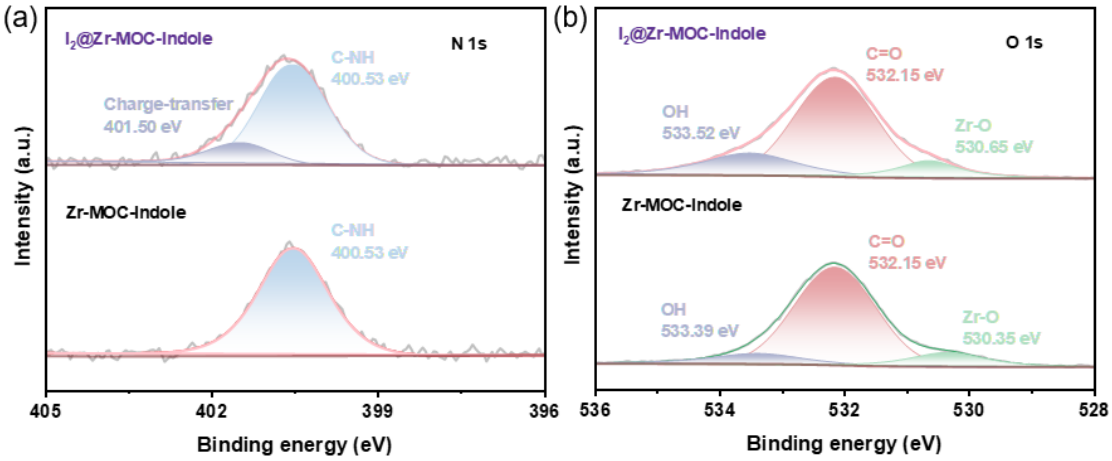

Fig. S15. N 1s, O 1s, and I 3d XPS spectra of Zr-MOC-Indole before and after iodine adsorption.

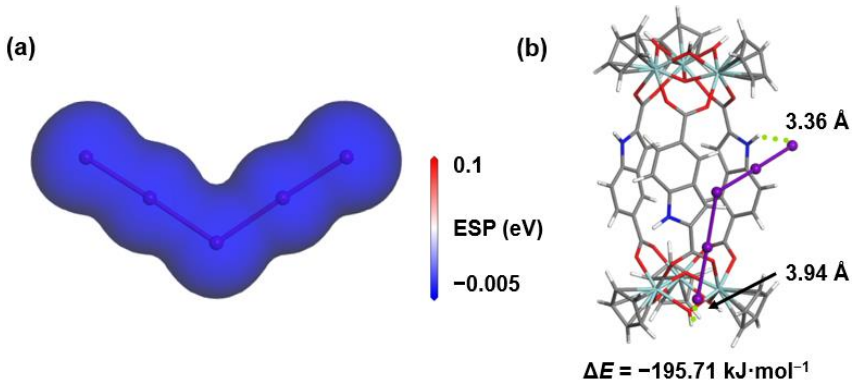

Fig. S16. (a) Electrostatic potential diagram and (b) the minimum binding energy site of I_5^-.

Table S1 Crystal data and structure refinement for Zr-MOC-Indole.

Compound	Zr-MOC-Indole
Chemical formula	$C_{101.4}H_{134.8}Cl_2N_4O_{40.7}Zr_6$
Formula weight	2679.14
Crystal system	monoclinic
Space group	$P2_1/n$
a/Å	23.1003(6)
b/Å	14.9053(3)
c/Å	27.9120(6)
α/°	90
β/°	92.428(2)
γ/°	90
V/Å^3	9601.9(4)
Z	4
ρ_{calc} g·cm^{-3}	1.853
μ/mm^{-1}	0.784
F(000)	5483.0
Data/restraints/parameters	24541/986/1067
Goodness-of-fit on F^2	1.034
Final R indexes [I>=2σ (I)]	R_1 = 0.0553, wR_2 = 0.1500
Final R indexes [all data]	R_1 = 0.0815, wR_2 = 0.1687
CCDC	2494240

Table S2 Kinetic parameters for iodine vapor adsorption by Zr-MOC-Indole.

Kinetics model	Parameters		R^2
Pseudo-first-order	0−4 h	$k_{1\text{-}1} = -0.141\ h^{-1}$	0.981
	5−10 h	$k_{1\text{-}2} = -0.193\ h^{-1}$	0.956
Pseudo-second-order	5−12 h	$k_2 = 0.287\ g\cdot(g\cdot h)^{-1}$	0.993

Table S3 Kinetic parameters for iodine adsorption in iodine/cyclohexane solutions (300 ppm) by Zr-MOC-Indole.

Kinetics model	Parameters	R^2
Pseudo-first-order	$k_1 = 0.210\ h^{-1}$	$R^2 = 0.967$
Pseudo-second-order	$k_2 = 8.359\ g\cdot(g\cdot h)^{-1}$	$R^2 = 0.991$

Reference

1. O. V. Dolomanov, L. J. Bourhis, R. J. Gildea, J. A. K. Howard and H. Puschmann, *J. Appl. Crystallogr.*, 2009, **42**, 339-341.
2. G. Sheldrick, *Acta Crystallogr., Sect. A*, 2015, **71**, 3-8.
3. G. Sheldrick, *Acta Crystallogr., Sect. C*, 2015, **71**, 3-8.
4. M. I. Jürg Hutter, Florian Schiffmann, Joost VandeVondele, *Wires Comput. Mol. Sci.*, 2014, **4**, 15-25.
5. S. Grimme, J. Antony, S. Ehrlich and H. Krieg, *J. Chem. Phys.*, 2010, **132**, 154104.
6. J. VandeVondele and J. Hutter, *J. Chem. Phys.*, 2007, **127**, 114105.
7. M. Dalapati, A. Das, P. Maity, R. Singha, S. Ghosh and D. Samanta, *Inorg. Chem.*, 2024, **63**, 15973-15983.
8. B. Xue, Y. Lv, W. Xuan, W. Zhu, Z. Li, L. Zhang and J.-Q. Wang, *J. Colloid Interface Sci.*, 2025, **692**, 137515.
9. W.-Y. Pei, J. Yang, H. Wu, W. Zhou, Y.-W. Yang and J.-F. Ma, *Chem. Commun.*, 2020, **56**, 2491-2494.
10. J. Wang, M. Chen, H. Zhao, Q. Dong, M. Wang, Z. Wu, W. Zhong, X. Li, D. Liu, T.-Z. Xie, Y. Li, P. Wang and Z. Jiang, *Langmuir*, 2023, **39**, 7337-7344.
11. Z.-Y. Zeng, Z.-C. Lou, L. Hu, W. Dou, X. Zhao, X. Li, J. Fang, X. Qian, H.-B. Yang and L. Xu, *Chem. Eng. J.*, 2024, **496**, 154091.
12. J.-Y. Liu, T.-P. Sheng, C. Li, Z. Wang, F.-R. Dai and Z.-N. Chen, *Cryst. Growth Des.*, 2022, **22**, 3182-3189.
13. M. Dalapati, R. Singha, P. Maity, D. Manna and D. Samanta, *Small*, 2025, **21**, 2504242.